MOLECULAR MECHANISM OF HEMOLYTIC ANEMIA IN HOMOZYGOUS HEMOGLOBIN C DISEASE

ELECTRON MICROSCOPIC STUDY BY THE FREEZE-ETCHING TECHNIQUE*

BY LAWRENCE S. LESSIN,‡ M.D., WALLACE N. JENSEN, M.D., AND ERIC PONDER, M.D.

(From the Institut de Pathologie Cellulaire, Kremlin Bicetre, France, and the Department of Medicine, Ohio State University College of Medicine, Columbus, Ohio)

(Received for publication 13 March 1969)

The substitution of lysine for glutamic acid in the sixth position of the hemoglobin beta chain is the single molecular aberration in homozygous hemoglobin C disease (2) and must account for the mild hemolytic anemia, splenomegaly, target cells, microspherocytes, (3, 4, 5) and the rare crystal-containing cells seen in this disorder (3, 6). Studies of the physical properties of erythrocytes from patients with homozygous hemoglobin C disease by Charache and coworkers have demonstrated decreased solubility of intracellular hemoglobin C (relative to hemoglobin A) (7). They suggest that abnormally tight molecular packing and altered molecular interaction may result from the substitution of lysine for glutamic acid in an exterior region of the beta chain, conferring a local difference in charge and, possibly, steric conformation. By increasing intramolecular attraction and fit, these alterations decrease solubility of hemoglobin C, which in turn leads to increased viscosity and decreased deformability of C-C erythrocytes as compared to normal cells. These factors produce accelerated erythrocyte "senescence" by reticuloendothelial pitting and fragmentation with the production of microspherocytes and crystal cells which are sequestered in the microcirculation and destroyed by reticuloendothelial elements.

Electron microscopic freeze-fracture-replication techniques appear to be capable of demonstrating hemoglobin molecules *in situ* in the erythrocyte (8–12). Particles of 65–70A have been identified in intraerythrocytic rat hemoglobin crystals (11), in the cytoplasm of rat erythrocytes, and in helical polymers of hemoglobin S *in situ* in sickled erythrocytes (12). The present study attempts to gain morphological insight into abnormal interaction of hemoglobin C molecules in C-C erythrocytes by employing an in vitro system of gradual osmotic dehydration for production of crystal cells (7), and the freeze-etching technique for preparation for electron microscopy (13).

Results suggest that hemoglobin C molecules exist intracellularly in a par-

* A portion of this work has been published in abstract form (1).

‡ Recipient of National Heart Institute Special Fellowship 1-F3-HE 35, 777-01.

Present Address: Duke University Medical Center, Durham, N. C.

tially aggregated state and that gradual water loss from C-C erythrocytes leads to a progressive decrease of intermolecular distance producing precrystalline molecular alignment and, finally, crystal formation.

Materials and Methods

Preparation of Crystal Cells.—Blood obtained by venopuncture from a 28 year old Negro male with homozygous hemoglobin C disease was drawn directly into heparinized blood bank tubing which was promptly heat-sealed and kept at low temperature until use. After 1–3 days storage, cells were washed twice in phosphate-buffered saline (NaCl, 8 g/liter; KCl, 0.3 g/liter; Na_2HPO_4, 0.184 g/liter; KH_2PO_4, 0.02 g/liter; glucose, 2.0 g/liter) buffered to pH 7.45. Samples taken after 4, 12, and 24 hr incubation were inspected with a Zeiss photomicroscope adapted for phase contrast, interference, Soret absorption, and polarization microscopy. "Unincubated" specimens were treated only by immersion in 25% glycerine in phosphate-buffered normal saline to prevent formation of ice-caused artifacts and disruption of cells during freezing. Samples were centrifuged at 1200 rpm for 5 min and cells resuspended in 25% glycerine in phosphate-buffered saline for 20 min.

Freeze-Etching.—Droplets of the glycerinated, centrifuged "crystal cell" preparations (from 0, 4, and 12 hr samples) were placed on centrally scratched 3 mm copper discs and immersed successively into liquid dichloromonofluorethane (−150°C) and liquid nitrogen (−196°C). The discs bearing the frozen droplets were then placed on the liquid nitrogen-cooled stage of a Balzers 500M high vacuum plant with freeze-etching device and freeze fractured with platinum-carbon replication carried out by the method of Moor and Muhlethaler (13). Replicas thus obtained were cleaned of adherent cells and fragments by successively floating on commercial bleach and 70% sulfuric acid, and they were triple-washed in distilled water. They were then placed on neoprenized 200-mesh copper grids and viewed with Philips EM-200 and Associated Electronic Industries EM-6B electron microscopes.

Reflection Densitometry of Electron Micrographs.—Reflection densitometry of electron micrographs was carried out with a Photovolt Reflection Density Unit (Model 53) and photometer (501A). Strips, 3 cm wide, of electronmicrographs of magnifications from 179,000 to 217,000 were scanned by the 0.40 cm spot at 0.25 cm intervals, with light incident at 45°. Readings were given in units of "reflection density", defined as $\log_{10}(R_o/R_t)$ where R_o is the light reflected by a white surface and R_t that reflected by the test surface. Tracings, except in one test case, were made parallel to the shadowing direction of the replica. Mean reflection densities and their standard deviations were used as a measure of uniformity of a given electron micrograph; more specifically, here, these data are used to compare variations of homogeneity in portions of two adjacent cells in the same micrograph. Because the size of the scanning spot exceeded that of the interval scanned, the curves do not reflect minute variations in density, but represent an integration of density maxima and minima, relating respectively to interaggregate spaces and particle aggregates.

Correction of Dimensional Distortion Produced by the Replication Process.—The correction system used is adapted from that of Misra and Das Gupta, (14) calculated for heavy metal shadowing of specimens of known size, including latex and colloidal gold particles. The system permits correction of distortions due to shadowing angle and variations in heavy metal deposition if the shadowing angle is known.

Schema I indicates the basic trigonometric method used, where θ is the shadowing angle (in our case, always 45°) AB, the true height diameter of the particle in a plane perpendicular to the horizontal (the fracture plane) and AC = EF, the measured "height" of the structure. Hence, $AB = AC \cos \theta$.

Schema II shows the techniques for correction of width diameter, d, of a spherical particle

where measured width, d, (perpendicular to the shadowing direction, arrow) and shadow length, l, are determined from the electron micrograph, and shadowing angle θ is known (45°).

It has been shown that the relationships of shadowing angle, θ, particle diameter, d, and shadow length, l, are given by the formula:

$$\text{Tan } \theta = \frac{d(l - d/2)}{l(l - d)}$$

From this, one can determine d as given by:

$$\Delta d = d' - d = \frac{d' - (2(l)(\tan \theta))}{(l + \cos \theta)}$$

Since minor deviations of the fracture plane from the true horizontal and variation in heavy metal deposition determining the size of metal caps (shaded areas) could not be well controlled, the precision of these corrections is variable.

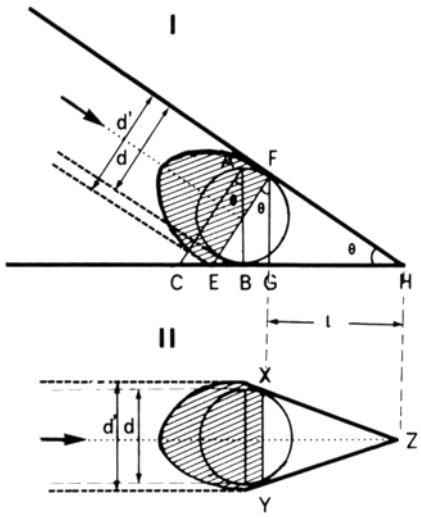

SCHEMATA I AND II.

Schema I shows the trigonometric correction of dimensional distortion due to shadowing, in lateral projection, where d' is the observed height of a shadowed sphere, and d the true height. Schema II shows the method used for correction of shadowing error in width, based on an empirical formula (see text). Adapted from Misra and Das Gupta (14).

RESULTS

Optical Microscopy.—C-C erythrocytes, after suspension for 20 min in the glycerine–normal saline solution at 37°C, showed minor morphologic alterations including spicule formation, and partial loss of target cell morphology (Fig. 3); microspherocytes showed no observable change. After 4 hr of dehydra-

tion by incubation in 3% NaCl solution, the C-C erythrocytes demonstrated shrinkage of cell contents into central masses surrounded by halos of membrane. Some central masses assumed polygonal form and showed weak birefringence. After 12 hr of incubation, 25 to 50% of the cells contained crystalloid inclusions, occasionally several in a single cell, in the form of hexagonal and tetragonal plates and prisms. Elongate crystals often produced marked distortion of the cell membrane by protraction about the extremities of the crystal. Crystalloid

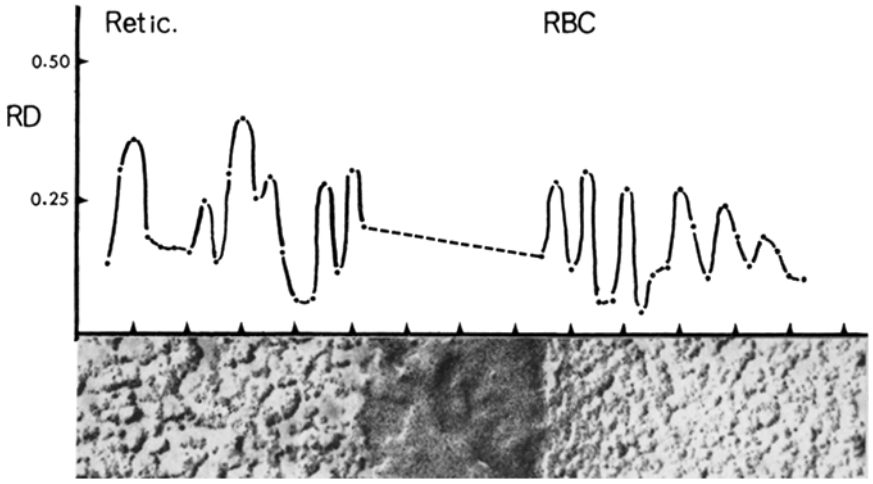

FIG. 1. Reflection densitometric curve of an electron micrograph strip of reticulocyte and adjacent erythrocyte replica from Fig. 5. Curves indicate increased peak frequency in the juxtamembrane regions of the erythrocyte (RBC) and the density irregularity of the aggregate meshwork in the reticulocyte with greater maximum-minimum distances. Reflection density (RD) with standard deviations, *P*-value and mean maximum-maximum, maximum-minimum distances are given in Table I.

inclusions uniformly showed negative birefringence (Fig. 4) and an angle of extinction (determined by rotating stage) of about 45°. Birefringence indicates noncubic molecular alignment within the crystals (15). Soret absorption (obtained by monochromating the cadmium arc light source with 415 mμ exclusion filter) by the crystalloid inclusions was strong, confirming a high concentration of heme-containing protein in the crystals.

Electron Microscopy.—Freeze-etched replicas of unincubated cells made after glycerinization in a medium, normotonic with respect to NaCl, showed generally rounded cell contours, although a few cells developed spicules (Fig. 3, 0 hr × 7000). Fracture planes passing through the cell interiors revealed relatively uniform coarse granular patterns. At high magnifications, this granular appearance was seen to be composed of aggregates of 2–10 closely applied 70 A

particles (Figs. 5 and 6). These aggregates were separated by spaces measuring up to 250 A. Average interaggregate spacing was greatest at the center of the cell interior and least adjacent to the cell membrane, where particles appeared more tightly packed, and in some juxtamembrane regions showed linear alignment. Although the majority of unincubated C-C cells showed relatively wide interaggregate spacing, rare cells showed packing of particles both in cell center and periphery. Reticulocytes encountered in these preparations (Fig. 6), identifiable by the presence of simple and autophagocytic vacuoles, showed greater interaggregate spacing and lesser aggregation of particles. In these cells, small aggregates 3 to 5 particles across, were distributed more or less uniformly throughout the cell interior, showing very little packing in the juxtamembrane regions.

Replicas of cells freeze-etched after 4 hr of hypertonic incubation showed greater variation in the granular patterns of their cytoplasm (Figs. 8 and 9). Adjacent cells, varying in degree of aggregation of cytoplasmic particles, were frequently encountered (Fig. 8). Microphotoreflectometry (Fig. 1) was used to quantitate size and statistical variation of this spacing within a given cell and in adjacent cells (see below).

Replicas of cells freeze-etched after 12 hr of incubation in hypertonic medium revealed the presence of polygonal inclusions in about 50–75% of erythrocytes included in the fracture plane. The remaining cells showed tighter packing of cytoplasmic particles with coalescence of particle aggregates and minimal interaggregate spacing. Again, packing of particles was most marked in the juxtamembrane regions where areas of linear alignment were found in the cell interior, well removed from visible membrane structures. Cells manifested a spectrum of variation in particle aggregation and spacing, with juxtamembrane regions consistently showing the tightest packing of particles.

Crystalloid inclusions showed characteristic polygonal contours. The presence and dimension of definable periodicity was dependent upon the direction of the fracture plane and the degree of etching (Figs. 10 and 11). Approximately one-third of these inclusions showed a simple linear and laminar periodicity of particles. The period was variable, measuring from 70–100 A (corrected). A few crystals permitted more detailed examination of the crystal structure and measurement of at least two dimensions of the molecular subunits (Fig. 11) and their mode of arrangement in the crystal lattice (see paragraph below on crystal structure).

Aggregation of Cytoplasmic Particles.—In none of the preparations were the 70 A cytoplasmic particles found completely dissociated from adjacent particles. Reticulocytes presented the least degree of particle aggregation and the greatest spacing. Except in the juxtamembrane areas, where some degree of packing was nearly always seen, the cytoplasmic particles were disposed in chains 1 to 5 particles thick, branching to adjacent chains to form a meshwork of chain-like

aggregates of particles interspersed with open spaces. These open spaces, regions relatively devoid of platinum-carbon deposition in the replica, are interpreted to represent, primarily, regions of depression between chains of particles from which water molecules were sublimated during the etching process, (16) and, secondarily, shadows of the particles and aggregates themselves. The chains, measuring from 70–350 A (corrected) are separated by open spaces up to 500 A (corrected) in width.

The other extreme of particle aggregation and packing was seen in 4 and 12 hr incubated specimens (rarely seen in unincubated ones) in which the chain-space meshwork coalesced into a more tightly packed, homogenous pattern. Juxtamembrane regions of tightly packed particles manifested varying degrees of organization and alignment (Fig. 8).

Intermediate stages showed coalescence of single and complex chains into larger aggregates with greater aggregation and tighter packing as dehydration progressed (Fig. 9).

Crystal Structure.—Crystalloid inclusions observed in C-C cells incubated in hypertonic medium for 12 hr and longer were negatively birefringent. Preparations further dehydrated between slide and cover slip overnight at 37°C developed many large extracellular crystals (measuring up to 100 μ) manifesting the same shape and birefringence as the smaller intracellular crystalloid inclusions (Fig. 4). Replicas of freeze-etched intracellular crystals revealed molecular subunit structure and manifested two patterns of periodicity. The pattern and period seen was dependent upon the direction of the fracture plane relative to the long axis of the crystal, and corresponded to the three-dimensional aspects of the crystal. Two distinct patterns were seen. The first was a linear-laminar period of 60–100 A (P_1) in which a single direction of alignment could be discerned. The second (P_2, Fig. 10), seen within the same crystals, was a 300–350 A period resembling sheets of juxtaposed layers composed of 70 A particles and appearing to represent fractured ends of laminae seen in pattern P_1 (Fig. 11). At higher resolution subunit particles measuring about 65 A by 100 A could easily be identified. These particles were arrayed in a noncubic monoclinic pattern resembling either a tetragonal or hexagonal arrangement, depending on the region of the crystal viewed (Fig. 11, *t* and *h*).

Comparison to Normal Erythrocytes.—A-A erythrocytes collected by venopuncture in heparin anticoagulant and subjected to osmotic dehydration, failed to show intracellular crystalloid inclusions during up to 72 hr of incubation at 37°C in a medium identical to that used for C-C cells. Moreover, the majority of the normal cells became crenated and hemolyzed, showing significantly less resistance to the hyperosmotic medium than the C-C cells. It was possible, however, to produce crystals in normal cells by simply allowing a drop of blood to air dry between slide and cover slip on the lab bench overnight; the degree of crystallization could be augmented by adding a drop of 1% sodium

bisulfite, thus increasing the proportion of methemoglobin; see Bessis, et al (17).

Replicas of normal erythrocytes, freeze-etched after washing and immersion in a mixture of 25% glycerine in phosphate-buffered (pH 7.4) normal saline show a number of significant differences from C-C cells. The aggregation-spacing phenomenon seen in replicas of the majority of freeze-etched C-C cells is much less apparent in the normal cells. The latter present, to a greater extent, the pattern of random dispersion found in the 70 A cytoplasmic particles. Although the particles appear less closely packed, regions of open-space measuring up to 150 A can be defined, distributed randomly throughout the cell interior, but excluding the juxtamembrane region. In this region, tight packing and a degree of alignment of particles similar to that seen in the C-C cells is commonly found. A few normal cells did present a picture of tight packing, both in the juxtamembrane region and throughout the cell interior, resembling the C-C cell preparation after 4 hr of hypertonic dehydration. This small proportion of normal cells did manifest aggregation of cytoplasmic particles, but to a lesser degree than their C-C counterparts. At no time, did replicas of freeze-etched normal cells show particulate alignment of a paracrystalline or crystalline type.

TABLE I

Reflection Densitometric Analyses

Figure	Subject	Magnification $\times 10^3$	Mean reflection density ± SD	Significance	Mean corrected maximum − maximum distance	Mean corrected minimum − maximum distance
7	RBC (perpendicular to shadowing)	217	0.46 ± 0.080*	$P < 0.1$	265 ± 85 A*	176 ± 60 A*
	Same RBC (parallel to shadowing)	217	0.25 ± 0.075		254 ± 60 A	107 ± 43 A
7	Reticulocyte	179	0.21 ± 0.095	$P < 0.025$	273 ± 106 A	178 ± 86 A
	RBC (adjacent to reticulocyte)	179	0.16 ± 0.078		293 ± 63 A	147 ± 84 A
5	RBC (*a*)	181	0.32 ± 0.145	$P < 0.005$	344 ± 87 A	244 ± 195 A
	RBC (*b*)	181	0.27 ± 0.056		365 ± 205 A	205 ± 58 A

* Standard deviation.

Reflection Densitometric Studies of Electron Micrographs.—Reflection densitometry was used in this study to assess density variation patterns per unit distance of a given electron micrograph. This distance measurement initially made in millimeters on the micrograph is easily converted to Angstroms of the replica. Fig. 1 is a representative study and points up several quantitative

aspects of the analysis which corroborates the qualitative impression of the micrograph strip (Table I). The reflection density curve for the reticulocyte (same as that shown in Fig. 6) shows a more marked variation of maxima and minima, with wider spacing of peaks in comparison to the older RBC on the right, where density variation and mean density are less. The curves, integrals by nature of the scanning technique, reflect the closer packing of particles and reduced interaggregate spacing in the juxtamembrane area. These integrated differences in density distribution of replicas of adjacent cells in the same electron micrograph confirm in quantitative terms visual impressions of interaggregate spacing, aggregate size, and particle packing gained from the micrographs. Table I presents data from such studies. The two scans of the same cell (in Fig. 8) in directions perpendicular and parallel to the shadowing direction are included to show the effect of shadowing direction of mean density and minimum-maximum spacing.The first measurements refer to the reticulocyte and RBC shown in Figs. 6 and 7; the third to adjacent erythrocytes in Fig. 9.

DISCUSSION

Cytoplasmic Particles and Hemoglobin Molecules.—The identification of the cytoplasmic particles characteristic of freeze-etched erythrocytes with hemoglobin molecules is based upon the presence of particles of identical size, 65–70 A (corrected), in intraerythrocytic crystals showing absorption in the Soret 412 mμ light band, specific for heme. Although particles of this type have not been visualized in red cells studied by standard electron microscopic techniques, due probably to the denaturation and polymerization of hemoglobin by aldehyde and osmic acid fixation,(18, 19) they are consistently present in freeze-fracture replicas of erythrocytes (8–12). In techniques in which a minimum of "etching" (removal of intermolecular and, possibly, intramolecular water from the fracture surface by sublimation in a high vacuum at low temperature) is employed, cytoplasmic particles are larger, 100–150 A (uncorrected), and more variable in size (8–10). The Moor-Muhlethaler technique (13) used in this study employs a 1 min sublimation at -100°C and 10^{-5} torr. The actual measurement of replica cytoplasmic particles is 90–100 A. Correction of this value by the method outlined above yields a value of 63–70 A, comparable to the X-ray diffraction measurements of Muirhead, Perutz, et al. for human oxyhemoglobin, 63.4 A × 83.6 A × 53.9 A (per unit cell of two molecules (20). Hemoglobin molecules identified in freeze-etched crystals of rat hemoglobin show similar dimensions, and 3 or 4 subunits of 20–35 A may be discerned in these molecules (11). Similar 65–70 A particles have been shown to organize into helical polymers in sickle cells freeze-etched after sickling with sodium bisulfite (12). Membrane associated particles (Figs. 3 and 5) vary in size from 65 A–150 A and from spherical to oval in shape. On internal erythrocyte membrane surfaces, such particles may be seen in continuity with those of the cytoplasm, and they are more uni-

form in size, measuring about 70 A. This relationship suggests that some internal surface particles may in fact be hemoglobin which remains adherent to the internal membrane surface when the remainder of the cytoplasm is fractured away. The external surface is more complex, manifesting a greater number and variation of particles which could represent structural proteins and antigenic glycoproteins (21).

Correlation of Morphologic and Biophysical Abnormalities in C-C Cells.— Peripheral blood films of individuals homozygous for hemoglobin C are composed predominantly of two cell types, the target cell and the microspherocyte. Reticulocytes, biconcave discs, and a variety of poikilocytes are present in relatively small numbers. Careful inspection of such films yields 2–5 per 1000 cells containing crystalloid inclusions (3, 6). In splenectomized C-C patients, the number of "crystal cells" may increase to 3% in dried films (6). After ultracentrifugal separation, Charache et al. found that the mean corpuscular hemoglobin concentration and viscosity were greater in the "older", more dense microspherocytes, which crystallized with less osmotic dehydration, than in the lighter, less viscous, "young" target cells (7). In addition, these authors found that the mean corpuscular hemoglobin concentration was greater in C-C target cells than in normal cells of comparable age. They found that whole blood viscosity was higher, and that C-C cells passed much less readily through 3 μ millipore filters. The latter finding suggests decreased deformability and increased rigidity of erythrocytes containing C-C hemoglobin as compared to those with A-A hemoglobin. Morphologically, the present study presents evidence for pathologic aggregation of hemoglobin C molecules within C-C cells, even at the reticulocyte stage. Aggregates form a meshwork, interspersed with spaces containing primarily water and electrolytes. This aggregation leads to a decrease in freedom of molecular movement, and thus an internal rigidity of C-C cells. This rigidity accounts for the increased mechanical fragility[1] of these cells (decreased ability to deform when compressed by glass beads) and decreased filtrability of such cells through millipore filters (7). Such rigid cells have been found to lose membrane by fragmentation in passage through the microcirculation. Simultaneously, the intracellular water content decreases as does the surface:volume ratio of the cell (22). In the present study, freeze-etched replicas of C-C cells in which water loss has been produced by gradual osmotic dehydration show a progressive increase in molecular packing, with concomitant decrease in intermolecular spacing, to the point where the intermolecular distance can no longer be resolved by this technique. Studies of low angle X-ray scattering by human red cells after incubation in normotonic, hypotonic, and hypertonic solutions suggest a mean (center to center) distance of 65 A for normal cells, 85 A in osmotically swollen cells, and 51 A in osmotically shrunken cells; i.e., a progressive decrease in intermolecular distance, and

[1] Lessin, L. S. Unpublished data.

increase in mean corpuscular hemoglobin concentration as intracellular water decreases (23). In osmotically dehydrated C-C cells, in the present study, it appears that not only do hemoglobin molecules approximate into a tightly packed system, but when a critical level of packing is achieved, alignment of molecules begins, initially in the juxtamembrane region, and subsequently in nidi within the cell interior. This may represent a precrystalline alignment and give rise to very small, rigid paracrystals, which by virtue of their surface location, can be "pitted" from these cells within the splenic microcirculation by a mechanism analogous to that described for Heinz bodies (24). With further loss of intracellular water, and consequent tighter packing of molecular aggregates, a second critical decrease in intermolecular distance occurs, that which corresponds to solubility saturation point of hemoglobin C, and crystallization takes place. These crystal cells appear to be extremely short-lived in the patient, probably destroyed in a single passage through the microcirculation, since very few circulation "crystal cells" can be found in dried peripheral blood films of nonsplenectomized C-C patients and, after splenectomy, they may increase to as high as 3% (6). In a single passage through a 3 μ millipore filter in normotonic buffer, 83% of C-C cells become entrapped in the filter mesh, whereas only 47% normal cells fail to cross the filter. This difference is accentuated when cells are rendered more rigid by osmotic dehydration (7).

A Molecular Model for the Pathological Behavior of Hemoglobin C-C Erythrocytes.—Aggregation, precrystalline alignment, and intracellular crystallization of hemoglobin C molecules appear to be the characteristic fine structural abnormalities of hemoglobin C molecules observed in freeze-etched preparations of serially dehydrated C-C erythrocytes. Moreover, this pathological behavior must derive directly from the anomaly of primary structure of hemoglobin C, namely, the substitution of lysine, with its two amino groups and net positive charge, for glutamic acid, a dicarboxyl amino acid with net negative charge (2). The external position of the positively charged polar group in the A-helix of the beta chain, distant from areas of intramolecular alpha-beta interaction, makes this site readily available for formation of a polar bond with a negative external site for an alpha chain of a neighboring hemoglobin C molecule (cf. Perutz and Lehmann (25), once a critical intermolecular distance is overcome. Thus, pathological polymerization accounts for the increase in red cell rigidity encountered in C-C erythrocytes. This progresses from an aggregation meshwork in young cells to crystallization in the aging cell which, by symmetrical loss of membrane lipid (26) decreases its surface to volume ratio, loses intracellular water (22), and reduces intermolecular distance. A comparable mechanism of hemolysis has been described for the rat paracrystalline erythrocyte (27), in which hemoglobin exists in a "metastable state of incipient crystallization" (28). In sickle cells hemoglobin S molecules polymerize into a six-stranded helix (29, 12) rather than a crystal, similarly a function of alteration of primary structure of

the beta chain of globin. At position 6 of the hemoglobin S beta chain, valine replaces glutamic acid. It is suggested that this gives rise to 1-6 valo-valoyl hydrophobic bonding in the A-helix region of the beta chain, a tertiary structural alteration which permits linear stacking of hemoglobin molecules into monomolecular filaments (12). These in turn twist into six-stranded helices (29, 12). Perutz and Lehmann (25) have suggested that in heterozygous hemoglobin S-A, the presence of hybrid molecules may limit the growth of such polymers by terminating the monomolecular filaments with the beta chain of hemoglobin A which lacks the necessary tertiary alteration to permit further

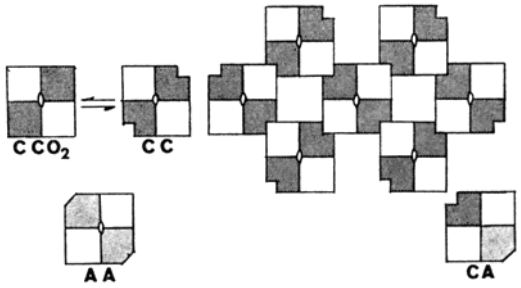

FIG. 2. A hypothetical scheme for pathological polymerization of hemoglobin C-C molecules (after Lehmann and Perutz for hemoglobin S (25)). The beta-6-lysine for glutamic acid substitution in hemoglobin C confers a charge alteration in the external A-helix region of the beta chain (shaded portion) increasing intermolecular attraction. Deoxygenation ($CC\text{-}O_2 \rightarrow CC$) would produce further steric alteration favoring intermolecular fit. Molecular aggregation and crystallization as observed in C-C erythrocytes would result. Hemoglobin A-A and hybrid C-A molecules would not fit into the aggregation pattern or crystal lattice and thus sterically inhibit the process.

stacking. In a similar fashion, polymerization of hemoglobin C molecules in the heterozygous state could be limited by the presence of such $\alpha_2^A\beta^C\beta^A$ hybrids (see Fig. 2). There is, however, little chromatographic evidence for the existence of such molecular hybrids in heterozygous subjects.

The Artefact Question.—Freeze-fracture-replication techniques have been developed to circumvent artifacts of chemical fixation and dehydration (13). Aldehyde fixation acts by polymerization of proteins (18) and has been shown to markedly reduce the quantity of helix present in red cell membrane protein as does osmic acid (19). Yet in avoiding chemical artifacts, freeze-fixation introduces the possibility of physical artifacts related to molecular rearrangement or interaction due to rapid temperature descent. The chief argument against significant or irreversible alteration has been the postthawing viability of control cells or tissue after treatment with a suitable cryoprotective agent (16) such as glycerol or dimethylsulfoxide. The prevention of freeze-thaw hemolysis by such agents is well established and forms the basis for current methods of

cryopreservation of erythrocytes (30, 31). Studies of the effects of rate of freezing and concentration of glycerol on the survival rate of yeast cells indicate optimum viability with 20% glycerol at very slow (0.01°C/sec) rates, or at the rapid rates (−100°C/sec) employed in freeze-etching where "vitrification", the amorphous crystallization of water without formation of ice crystals, occurs (16). It must be asked, however, whether the aggregation or even crystallization of hemoglobin C molecules observed in the present study may be induced by the freezing process. Against this is the finding that similar aggregation and crystallization is not seen in preparations of normal human erythrocytes. Rat erythrocytes show intracellular crystallization but do not exhibit molecular aggregation (11). Sheep cells, freeze-cleaved after treatment with 40% glycerine, contain areas of periodic alignment of cytoplasmic particles but crystallization has not been described (10). Normal erythrocytes or those containing abnormal hemoglobins will exhibit intracellular crystallization on slow cooling to 4°C particularly when methemoglobin formation has occurred (17). The hypertonic crystallization system employed in the present study has been shown to be temperature dependent, with a 37°C optimum, and crystals can readily be identified with the optical microscope before the cells are frozen, whereas at 4°C, no crystallization occurs in the 12 hr incubation period.

The relation of molecular aggregation to freezing is more difficult to define. It has been recently shown that freezing can induce intermolecular disulfide bond formation in thiogel (32); glycerol appears to inhibit this phenomenon (33). In hemoglobin solutions, however, both hemoglobins A and S show decreases in the number of disulfide bonds on cooling from 38°C to 0°C, (34) whereas hemoglobin C shows a decrease in titratable sulfide groups consistent with the formation of inter- or intramolecular disulfide linkages (35).

SUMMARY

Erythrocytes from a patient with homozygous hemoglobin C disease were subjected to gradual osmotic dehydration by incubation in hypertonic saline. Serial observations of these cells before and after 4 and 12 hr incubation were carried out by means of interference, Soret absorption, polarization microscopy, and the electron microscope employing the freeze-etching technique. Light microscopic studies showed a progressive contraction of cellular contents into central masses which, after 12 hr dehydration, formed birefringent intracellular hemoglobin crystals in 50–75% of the cells. Electron microscopic study of freeze-etched replicas of these cells at 0, 4, and 12 hr of dehydration reveals progressive aggregation, alignment, and crystallization of hemoglobin molecules. Molecular aggregation found in C-C cells prior to osmotic dehydration was not seen in normal erythrocytes. Aggregation and packing varied from cell to cell. Reticulocytes showed a loosely packed aggregate mesh-work; older cells showed variation of molecular packing, which appeared tightest in cells corresponding to microspherocytes. With further loss of intracellular water, aggregates coalesced into patterns of tighter molecular packing with small regions of align-

ment, and, finally, crystallization occurred. Hemoglobin molecules measuring 70 A in diameter were readily identified within the period patterns of intracellular crystals. These findings suggest that the hemoglobin C molecules within C-C erythrocytes exist in an aggregated state. As the cell ages, intracellular water is lost and intermolecular distance decreases, hemoglobin C molecules polymerize into intracellular crystals. This pathological behavior of hemoglobin C is associated with a charge alteration conferred by the substitution of beta-6-lysine for glutamic acid on the external surface in the A-helix region of the beta-chain of the molecule, possibly increasing intermolecular attraction. Molecular aggregation accounts for the increased rigidity of C-C cells which leads to accelerated membrane and water loss with resultant microspherocyte formation. The microspherocyte, with highest intracellular hemoglobin concentration, rapidly undergoes intracellular crystallization, and is sequestered and destroyed by reticuloendothelial elements.

BIBLIOGRAPHY

1. Lessin, L. S., W. N. Jensen, and F. Padilla. 1968. Molecular rearrangement in intraerythrocytic crystallization in Hemoglobin C disease. *Clin. Res.* **16**:307.
2. Hunt, J. A., and V. M. Ingram. 1958. Allelomorphism and the chemical differences of the human haemoglobins A, S, and C. *Nature (London).* **181**:1062.
3. Wheby, M. S., O. A. Thorup, and B. S. Leavell. 1956. Homozygous Hemoglobin C disease in siblings; further comment on intraerythrocytic crystals. *Blood J. Hematol.* **11**:266.
4. Jensen, W. H., R. A. Schoefield, and R. Agnes. 1957. Clinical and necropsy findings in Hemoglobin C disease. *Blood J. Hematol.* **12**:74.
5. Smith, E. W., and J. R. Krevans. 1959. Clinical manifestations of Hemoglobin C disorders. *Bull. Johns Hopkins Hosp.* **104**:17.
6. Diggs, C. W., A. P. Kraus, D. B. Morrison, and R. P. T. Rudnicki. 1954. Intraerythrocytic crystals in a white patient with Hemoglobin C in the absence of other types of hemoglobin. *Blood J. Hematol.* **9**:1172.
7. Charche, S., C. L. Conley, D. F. Waugh, R. J. Ugoretz, R. J. Spurrell, and E. Gayle. 1967. Pathogenesis of hemolytic anemia in homozygous Hemoglobin C disease. *J. Clin. Invest.* **46**:1795.
8. Haggis, G. H. 1961. Electron microscope replicas from the surface of a fracture through frozen cells. *J. Biophys. Biochem. Cytol.* **9**:841.
9. Weinstein, R. S., and S. Bullivant. 1967. The application of freeze-cleaving techniques to red blood cell fine structure. *Blood J. Hematol.* **29**:780.
10. Weinstein, R. S., and F. B. Merk. 1967. Periodicity in the cytoplasm of freeze-cleaved sheep erythrocytes. *Proc. Soc. Exp. Biol. Med.* **125**:38.
11. Lessin, L. S. 1968. Structure moleculaire de l'hemoglobin cristallisée d'érythrocytes de rat, etudiée par cryodécapage. *Nouv. Rev. Fr. Hematol.* **8**:423.
12. Lessin, L. S. 1968. Polymerization hélicoidale des molecules d'hemoglobine dans les érythrocytes falciformes. Etude par cryodécapage. *C. R. Hebd. Séances Acad. Sci. Paris.* **266**:1808.
13. Moor, H., K. Muhlethaler, H. Waldren, and A. Frey-Wysling. 1961. A new freezing-ultramicrotome. *J. Biophys. Biochem. Cytol.* **10**:1.

14. Misra, D. N., and N. N. Das Gupta. 1966. Distortion in dimensions produced by shadowing for electron microscopy. *J. Roy. Microsc. Soc.* **84**:373.
15. Fulton, C. C. 1961. Observing microcrystals. *In* The Encyclopedia of Microscopy. Reinhold Publishing Corp., New York. 51.
16. Moor, H. 1965. Freeze etching. *Balzers Vacuum Report.* **2**:1.
17. Bessis, M., G. Nomarski, J. P. Thiery, and J. Breton-Gorius. 1958. Etudes sur la falciformation de globules rouges au microscope polarisant et au microscope électronique. *Rev. Hematol.* **13**:270.
18. Bowes, J. H., and C. W. Cates. 1965. The reaction of glutaraldehyde with proteins and other biological materials. *J. Roy. Microsc. Soc.* **85**:193.
19. Lenard, J., and S. J. Suyer. 1968. Alteration of the conformation of proteins in red blood cell membranes and in solutions by fixatives used in electron microscopy. *J. Cell. Biol.* **37**:117.
20. Muirhead, H., J. M. Cox, L. Mazzarella, and M. F. Perutz. 1967. Structure and function of Hemoglobin. III. A 3-dimensional Fourier synthesis of human deoxyhemoglobin at a 5.5Å level of resolution. *J. Mol. Biol.* **28**:117.
21. Staehelin, L. A. 1968. The interpretation of freeze-etched artificial and biological membranes. *J. Ultrastruct. Res.* **22**:326.
22. Danon, D. 1966. Biological aspects of red cell aging. Proceedings of the Eleventh International Congress of Hematology. University of Sidney, Sidney, Australia. 394.
23. Bateman, J. B., S. S. Hsu, Knudsen, J. P., and K. L. Yudovitch. 1953. Hemoglobin spacing in erythrocytes. *Arch. Biochem. Biophys.* **45**:411.
24. Rifkind, R. A. 1965. Heinz body anemia: an ultrastructural study. II. Red cell sequestration and destruction. *Blood J. Hematol.* **26**:433.
25. Perutz, M. F., and H. Lehmann. 1968. Molecular pathology of human hemoglobin. *Nature (London).* **209**:902.
26. Weed, R. I., and C. F. Reed. 1966. Membrane alterations leading to red cell destruction. *Amer. J. Med.* **41**:681.
27. Ponder, E. 1948. Hemolysis and Related Phenomena. Grune and Stratton, Inc., New York. 97–100.
28. Drabkin, D. L. 1945. Hemoglobin, glucose, oxygen and water in the erythrocyte. *Science (Washington).* **101**:445.
29. Murayama, M. 1966. Molecular mechanism of sickling. *Science (Washington).* **153**.
30. Doebbler, G. F., A. W. Rowe, and A. P. Rinfret. 1966. Freezing of mammalian blood and its constituents. *In* Cryobiology. H. T. Meryman, editor. Academic Press, Inc., New York. 407.
31. Meryman, H. T. 1966. Review of biological freezing. In Cryobiology. H. T. Meryman, editor. Academic Press, Inc., New York. 2.
32. Levitt, J. 1962. System for demonstrating intermolecular disulfide bond formation in freezing thiogel. *Cryobiology.* **1**:312–16.
33. Andrews, S., and J. Levitt. 1967. The effect of cryoprotective agents on intermolecular disulfide bond formation during freezing of thiogel. *Cryobiology.* **4**:85.
34. Murayama, M. 1957. Titratable sulfhydryl groups of normal and sickle cell hemoglobins at 0 degrees and 38 degrees. *J. Biol. Chem.* **228**:231.
35. Murayama, M. 1958. Titratable sulfydryl groups of hemoglobin C and fetal hemoglobin at 0 degrees and 38 degrees. *J. Biol. Chem.* **230**:163.

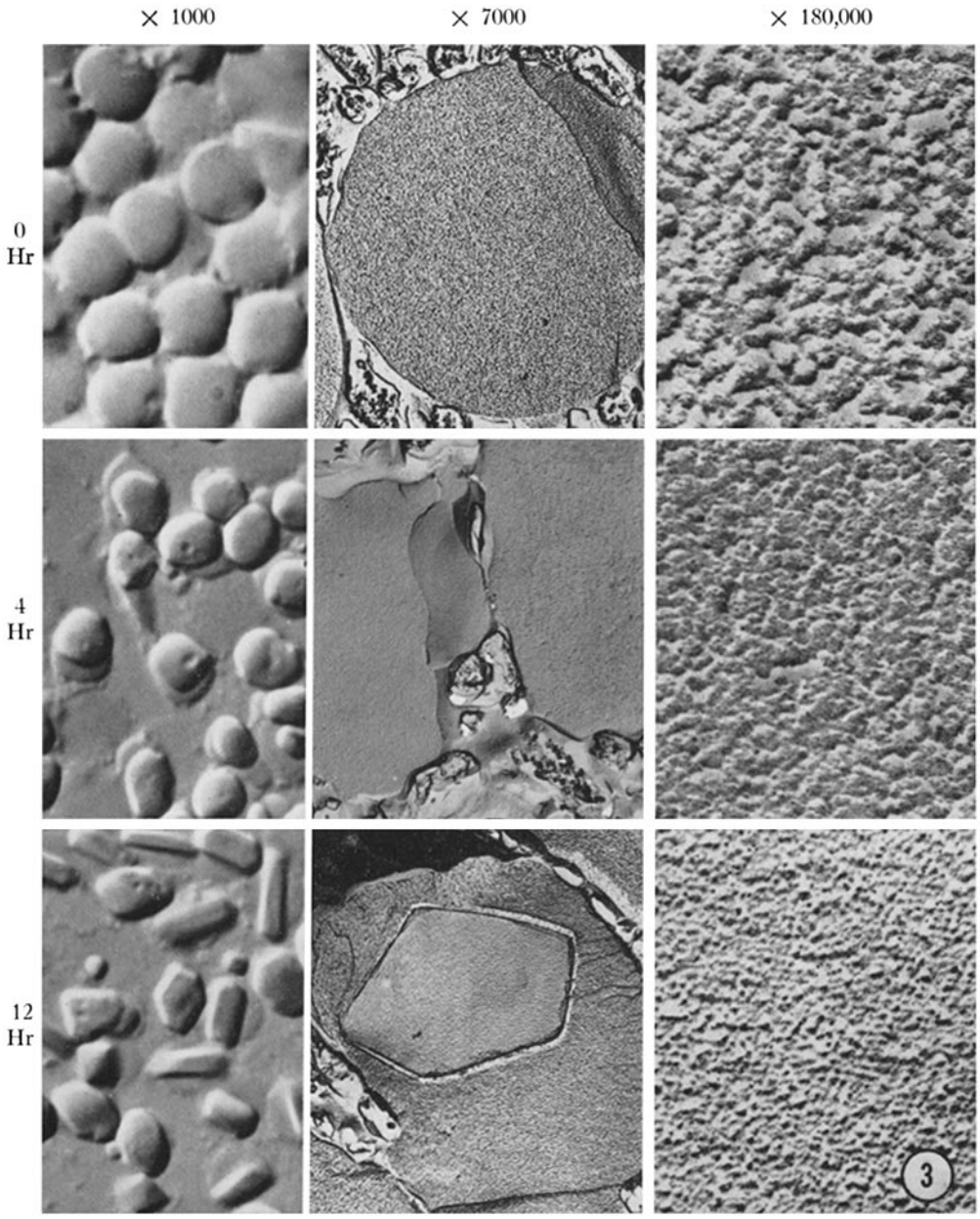

FIG. 3. Interference photomicrographs (× 880) and electron micrographs of freeze-etched replicas (× 6150 and × 158,000) of C-C erythrocytes prior to incubation in 3% saline (0 hr) and after 4 and 12 hr of hypertonic dehydration. Preincubation cells (0 hr) show rounded contours with some spicule formation. Freeze-etched replicas of these cells (× 6150) show coarse granularity in the cell interior which at 158,000 × is seen to be composed of a meshwork of aggregates on 70 A cytoplasmic particles interspersed with open spaces of varying size. After 4 hr of hypertonic dehydration, erythrocyte contents are contracted into central masses leaving peripheral membrane halos. Freeze-etched replicas of these cells show irregular borders and smoother, more homogenous appearance of the cell interior. At 158,000 ×, this is composed of tightly packed aggregates of 70 A particles with very little interaggregate spacing. After 12 hr of incubation, about 75% of the cells contain crystalline inclusions and membrane halos are visible about several crystals. Freeze-etching of this preparation reveals polygonal inclusions as shown which at 158,000 × can be seen to contain 70 A particles arranged in a noncubic crystal pattern.

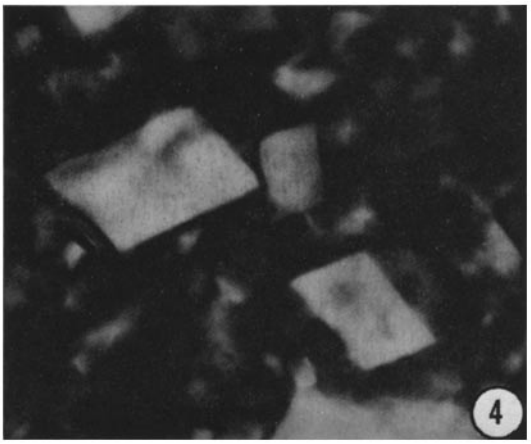

FIG. 4. Polarization photomicrograph of 24 hr incubation specimen of C-C cells showing multiple large birefringent extracellular crystals measuring up to 100 μ in length, and smaller, birefringent intracellular crystals. × 500.

FIG. 5. Freeze-etched replica of target cell surface from preincubation C-C cell preparation. Central mass and several punctate elevations are present on the membrane surface, which is characterized by a dense random distribution of 100–400 A round and ovoid surface particles. × 21,400.

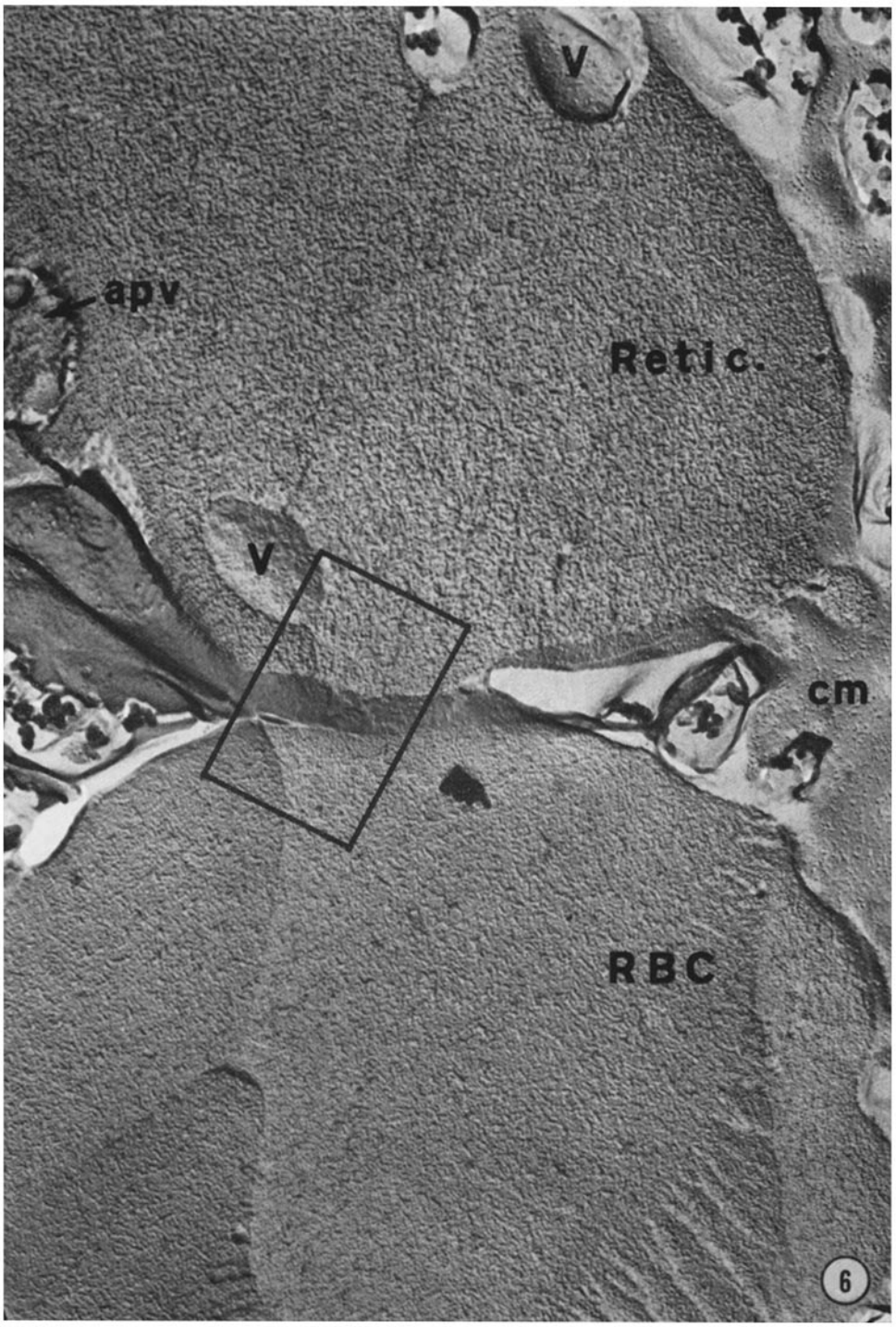

FIG. 6. Freeze-etched replica of C-C reticulocyte and erythrocyte prior to hypertonic incubation. Reticulocyte, identified by the presence of vacuole membranes (V) and autophagocytic vacuole (apv), shows loosely packed cell interior with slight difference between the juxtamembrane region and the cell center. Erythrocyte manifests tighter packing of cytoplasmic aggregates, and denser concentration of cytoplasmic particles in the juxtamembrane region. Portions of cell membrane (cm) may be identified. × 39,500.

FIG. 7. Magnified portion of Fig. 4 (rectangle) showing regions of reticulocyte (above) and erythrocyte (below) separated by cell membrane (cm) with its membrane associated particles (map). A fragment of membrane (*) from the lower cell remains. Reticulocyte, with portion of vacuole membrane (v), displays a loose meshwork of aggregates of 70 A cytoplasmic particles (agg) with relatively wide interaggregate spaces (ias) up to 500 A. Erythrocyte (below) shows tighter packing of aggregates and increased density of cytoplasmic particles (cp) in the juxtamembrane region (jmr). Some cytoplasmic particles are seen splayed out along the membrane-cytoplasm interface (× 260,000). A strip of this micrograph has been subjected to reflection densitometry for quantitation of density variation patterns of the two cells (See Fig. 10).

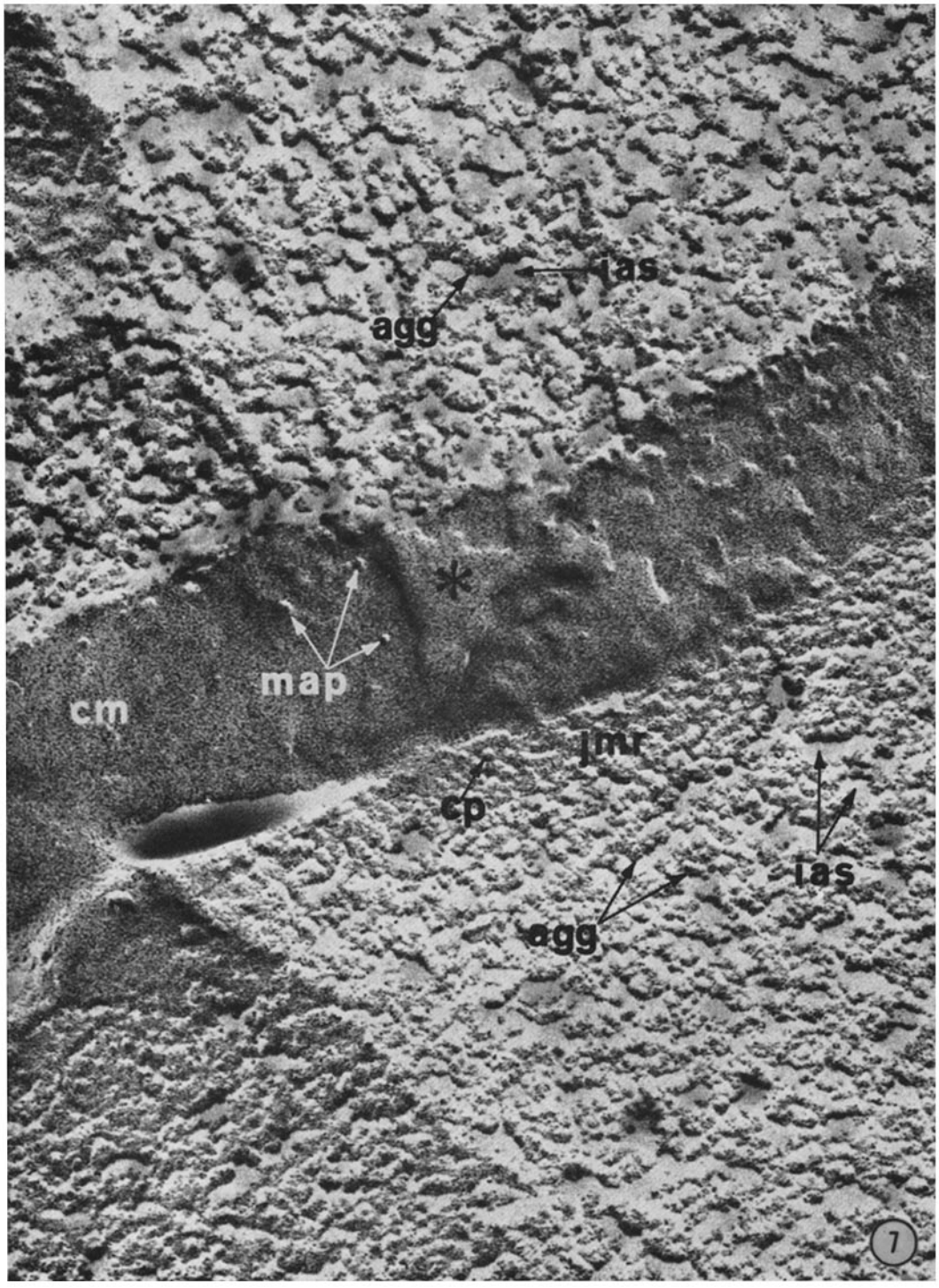
las
agg
*
map
cm
jmr
cp
las
agg
7

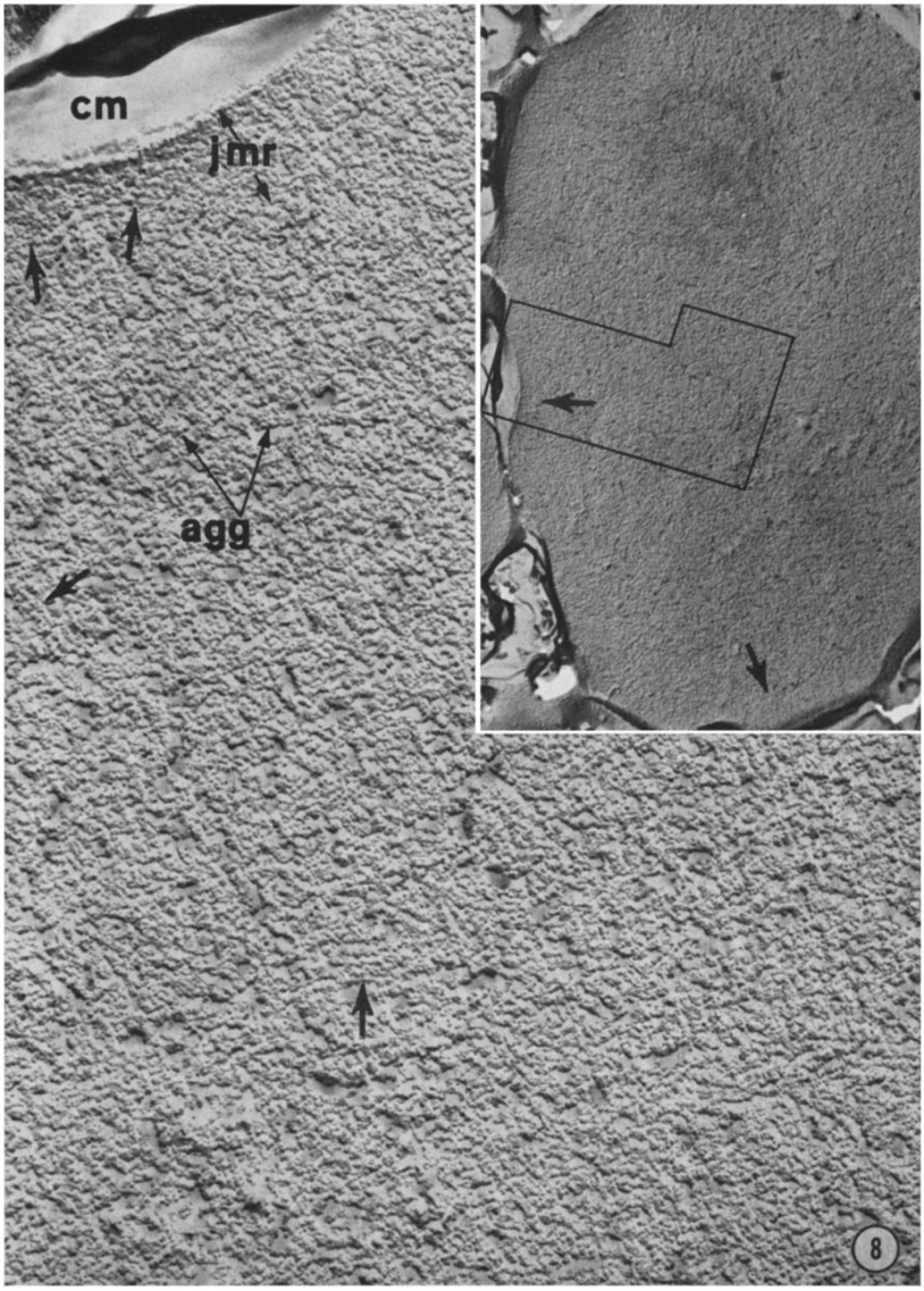

FIG. 8. C-C cell after 4 hr of hypertonic dehydration showing relatively smooth, homogenous appearance of cell interior (Inset, × 22,000). Magnified area (rectangle in inset) shows smooth cell membrane (cm), close packing of particles in juxtamembrane region (jmr), and aggregates (agg) more tightly packed than those of the preincubation erythrocyte and reticulocyte (Figs. 4 and 5). Many of the aggregates display alignment (arrows) of particles into chains and laminae (× 107,000).

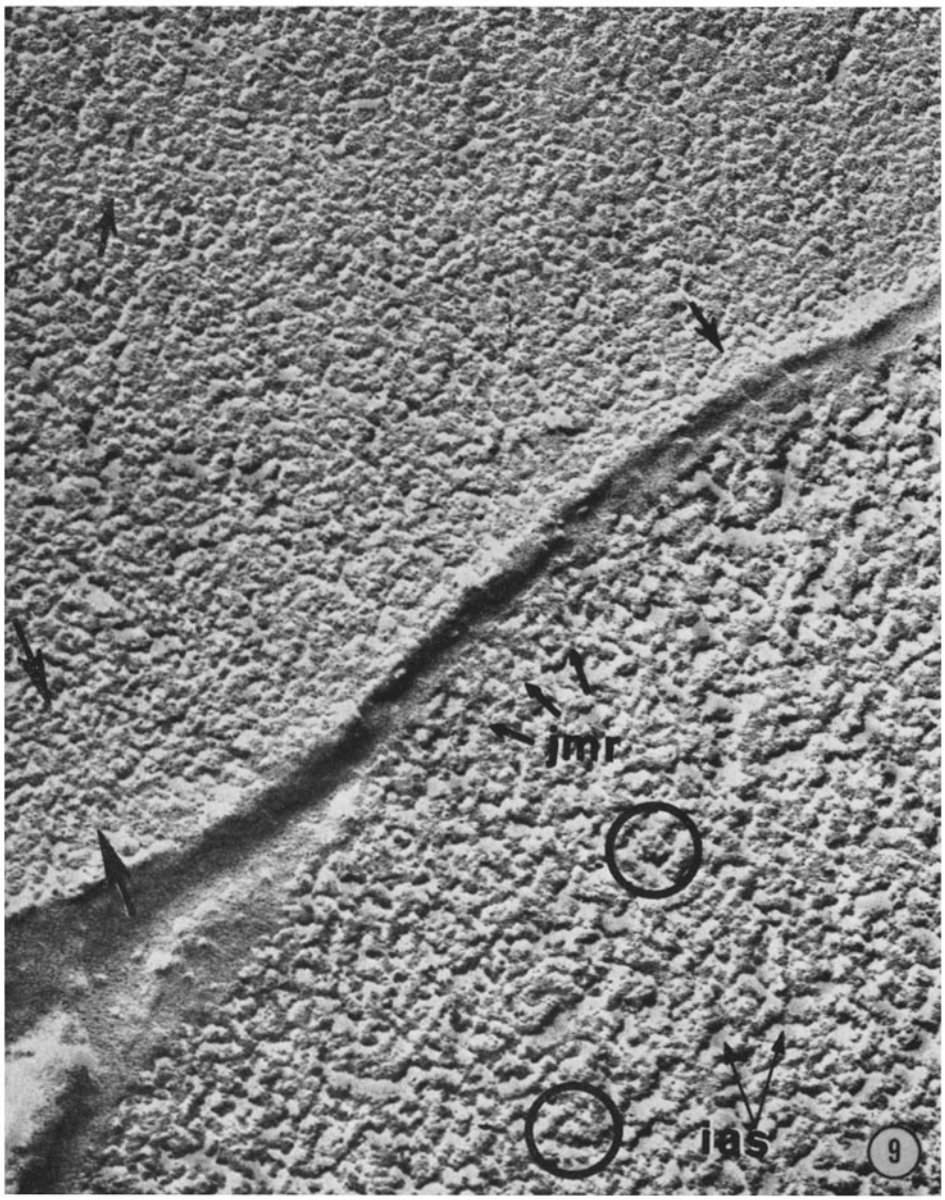

FIG. 9. Detail of replica of two C-C cells after 4 hr hypertonic dehydration. Upper cell segment shows tighter packing of cytoplasmic particles with areas of alignment (arrows). Lower cell segment shows detail of aggregates (circles) and interaggregate spaces (ias). Interaggregate spacing is reduced in the juxtamembrane region (jmr). × 109,000.

FIG. 10. Freeze-etched replicas of crystal cells after 12 hr of hypertonic incubation. 8*a* shows two crystal inclusions within a single erythrocyte. The upper crystal displays two patterns of periodicity (P_1, P_2, described in the text); the orientation of pattern P_1 is indicated by the heavy arrows. The particulate structure of the lower crystal shows no periodic arrangement. 8*b* is a portion of crystal cell demonstrating the relationship of pattern P_1 to pattern P_2 (8*a*, × 29,500, 8*b*, × 61,000).

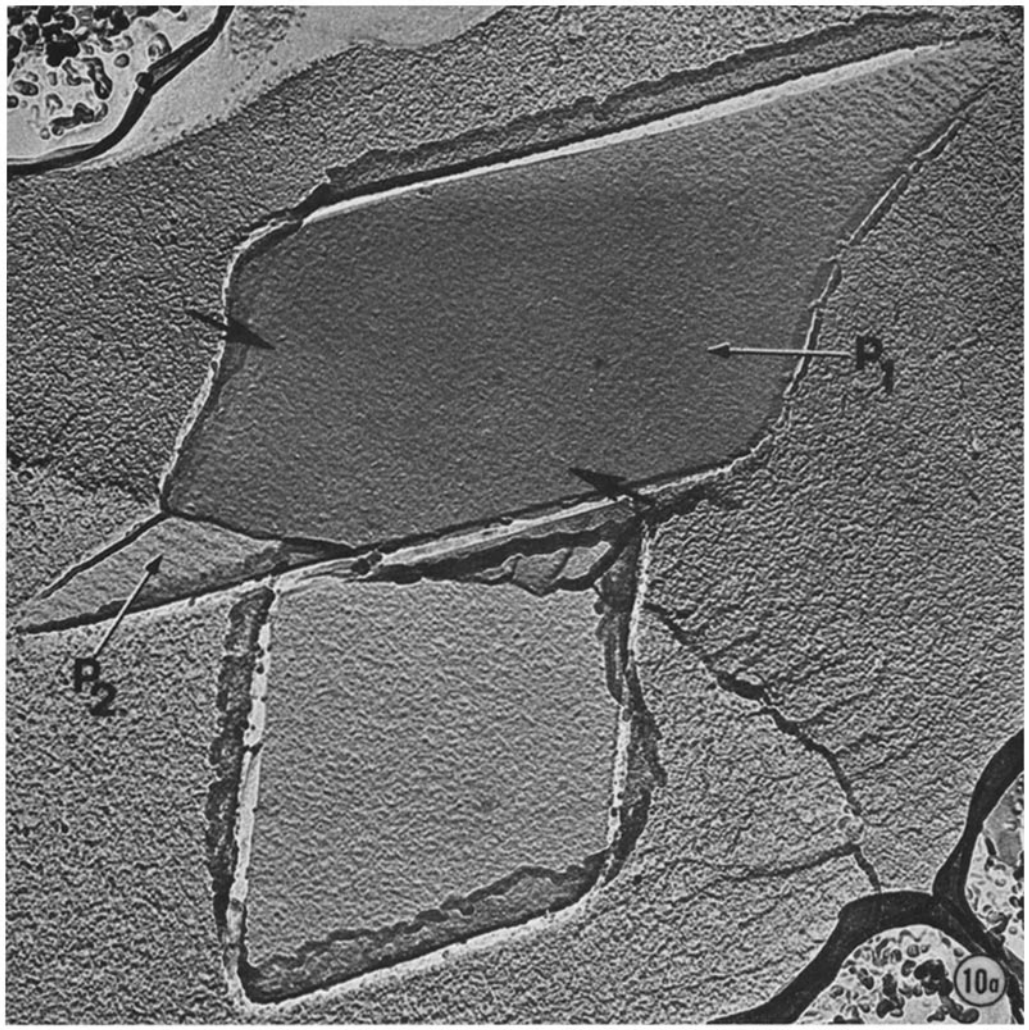
P1
P2
10a

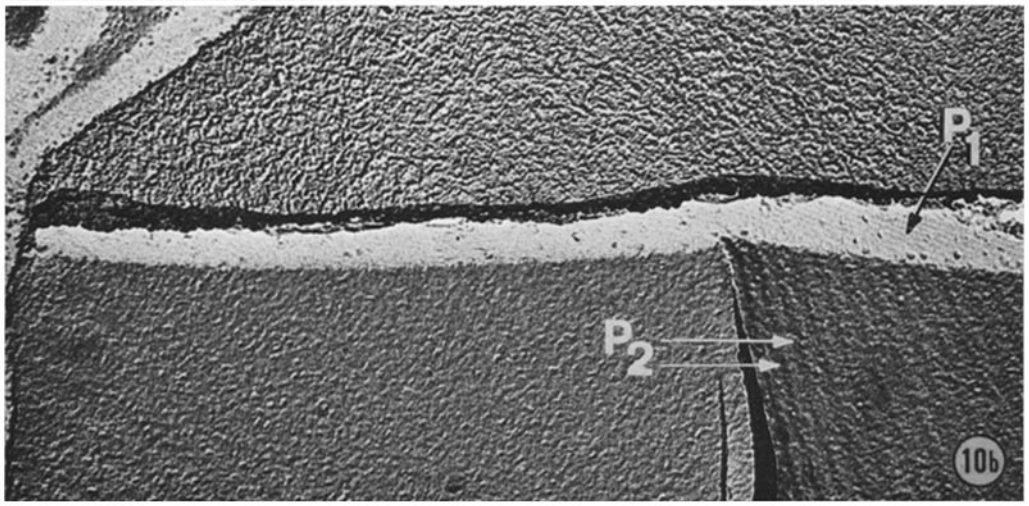
P1
P2
10b

FIG. 11. Freeze-etched replica of C-C crystal displaying the molecular subunit structure. The subunit arrangement is noncubic, P_1, appearing tetragonal (*t*) in some areas of the crystal and hexagonal (*h*) in others. In one portion of the crystal (upper right) fracture